Monte Carlo Simulation of Radiation in Gases with a Narrow-Band Model and a Net-Exchange Formulation :

Numerical Results for One Dimesionnal Configurations

CHERKAOUI Moha, DUFRESNE Jean-Louis,FOURNIER Richard,
GRANDPEIX Jean-Yves, LAHELLEC Alain

Laboratoire de Météorologie Dynamique , C.N.R.S-Université Paris 6,
F-75252 Paris Cedex 05, France

Internal Report N. 204 , june 1996

Additional results to the paper
"Monte Carlo Simulation of Radiation in Gases with a Narrow-Band Model and a Net-Exchange Formulation "
CHERKAOUI Moha, DUFRESNE Jean-Louis,FOURNIER Richard,
GRANDPEIX Jean-Yves, LAHELLEC Alain
published in
ASME Journal of Heat Transfer, May 1996, Vol.118, pp.401-407

Nomenclature, References, and Equation numbers are those of (Cherkaoui et al., 1996)

Except when otherwise stated all radiation budgets presented in the present section are computed with a statistical error lower than 1%. Radiation budgets generally have strong gradients close to the surface, therefore a rapidly varying discretization grid is used. The gas volume is symmetrically divided into 22 layers (Table 1). The two zero thickness layers enable the computation of the limit value of the radiation budget at the boundaries.

(a) High temperature configurations. Most benchmark configurations for gas radiative transfer are in the high temperature field. We give some results of EMCM simulations of such configurations before concentrating on room temperature configurations.

Radiation budgets in Table 2 correspond to slab thicknesses from $D = 0.01m$ to $1m$. Surfaces are at $\theta^s(1) = \theta^s(2) = 0K$ or $500K$ with emissivities $\epsilon = 1$, 0.5 or 0.1. The gas is isothermal at $\theta = 1000K$ and is either pure carbon dioxide or pure water vapor at atmospheric pressure. In order to allow comparisons with published results, some simulations where held where only one spectral band is considered : the $3755cm^{-1}$ band for water vapor (extending from $2875cm^{-1}$ to $4250cm^{-1}$) and the $3715cm^{-1}$ band for carbon dioxide (extending from $3275cm^{-1}$ to $3875cm^{-1}$). Radiative band parameters are those published in Hartman et al. (1984), Soufiani et al. (1985), and Zhang et al. (1988). The discretization is that of Table 1. Surface radiation budgets at the walls and volumetric radiation budgets in the central layers (average budget of the 11-th and 12-th layers) are given with a statistical error of the order of 0.1%. Our results are compatible (maximum 2% difference) with those published in Kim et al. (1991), Menart et al. (1993a and 1993b) and Liu and Tiwari (1994). As far as volumic radiation budgets are concerned, results match with those of Kim et al. (1991) within the plot reading precision.

(b) Room temperature configurations. We now turn to the main object of this work, namely the determination of volumetric radiation budgets in nearly homogeneous and isothermal cavities and the sensitivity analysis of these budgets to surface emissivities and absorbing gas concentrations. The following one-dimensional slab configuration is used which is an idealized representation of measured vertically stratified cavities with a hot ceiling and a cold floor. The gas temperature profile is taken linear from the cold surface temperature ($\theta^s(1) = 295K$ at $S(1) = 0$) to the hot one ($\theta^s(2) = 305K$ at $S(2) = D = 1m$). The gas is at atmospheric pressure and consists of one absorbing gas (carbon dioxide or water vapor) mixed with a non absorbing gas composed of 79% nitrogen and 21% oxygen (note that unrealistic water vapor concentrations will be considered, in order to compare CO_2 and H_2O radiative effects).

For water vapor narrow band parameters, the same data as before are used (Hartman et al., 1984 ; Soufiani et al., 1985 ; Zhang et al., 1988). For carbon dioxide, the available data in these three references do not include the $2350cm^{-1}$ band. We used more recent data (Soufiani, 1994).

Figures 1 to 5 display the radiation budget profiles for various carbon dioxide partial pressure ($P_{CO_2} = 1atm$ to $P_{CO_2} = 10^{-6}atm$) representative of the two classes of profiles corresponding to $P_{CO_2} > 10^{-3}atm$ and $P_{CO_2} < 10^{-3}atm$. The surfaces are diffuse reflective. Two symmetric cases ($\epsilon_1 = \epsilon_2 = 1$ and $\epsilon_1 = \epsilon_2 = 0.1$) are considered as well as a dissymmetric one ($\epsilon_1 = 0$; $\epsilon_2 = 1$). For $P_{CO_2} > 10^{-3}atm$, the profile has a pronounced "S" shape : the radiation budget rises significantly in the vicinity of the two surfaces (Fig. 6). In the center region, the radiation budget profile is approximately linear with values around a few $W.m^{-3}$ with small concentration dependence. For $P_{CO_2} < 10^{-3}atm$, the situation is very different. The radiation budget varies approximately linearly across the slab and is proportional to concentration. The two symmetric case profiles ($\epsilon = 1$ and $\epsilon = 0.1$) stay close to each other irrespective of the emissivity value whereas the dissymmetric case is strongly shifted.

In order to quantify these behaviors we performed a parameter sensitivity analysis which is presented in Figs. 7 and 8. Values of the volumetric radiation budget are looked at for two specific layers : the zero thickness one located along the cold surface ($\widehat{X} = 0$) and one located at about the fourth of the slab thickness ($\widehat{X} \approx 0.24m$).

Figure 7concerns symmetrical configurations with surface emissivities ranging from 0 to 1, for $P_{CO_2} = 10^{-4} atm$ and $P_{CO_2} = 10^{-1} atm$. The ratio between the radiation budget for surface emissivity ϵ and the radiation budget for black surfaces is plotted versus ϵ. For the low concentration case, this ratio is position independent and reaches 1.3 for perfectly reflective surfaces. In the high concentration case, the influence of surface emissivities is much greater and position dependent : the ratio takes values up to 2 at wall and 1.6 at center. In Fig. 8 the radiation budget is plotted versus partial pressure of the considered absorbing gas in the case of two diffuse moderately reflective surfaces ($\epsilon_1 = \epsilon_2 = 0.5$), with water vapor / air and carbon dioxide / air mixtures. Equivalent partial pressures of water vapor and carbon dioxide lead to radiation budget values of the same order of magnitude. For small concentrations the radiation budget is proportional to the partial pressure. For higher concentrations the proportionality is lost and the behavior is clearly different close to and far from the wall. Along the surface the radiation budget keeps increasing significantly with molar fraction, whereas it is nearly constant in the center region. These different evolutions at the wall and in the center region should be linked to the "S" shape observed at high concentrations. Similar results are obtained for other surface emissivities.

Table 3 gives the surface radiation budget of the hot surface for most configurations mentioned in this paragraph.

(c) About multiple reflections. Two questions are addressed in this paragraph : (i) the sensitivity of radiation budgets to the reflective properties of surfaces (diffuse or specular), (ii) the number of multiple reflections that need to be taken into account, to reach a given accuracy, as a function of absorber concentration. The same geometric and temperature configurations as in (b) are considered, with various P_{CO_2}.

To illustrate the first point, the ratio between the radiation budgets for diffuse and specular reflections is computed for each gas layer . In the case of one perfectly reflective surface and the other black ($\epsilon_1 = 0$, $\epsilon_2 = 1$), Fig. 9 displays the graph of this ratio versus P_{CO_2} for three specific gas layers : the zero thickness one located along the reflective surface, the one located approximately at 0.04m (layer 5) and the one located at 0.24m (layer 9). Along the reflective surface the ratio diffuse/specular starts at a value of one for extremely small concentrations of absorbing material and increases regularly with P_{CO_2}, up to 1.13 for pure carbon dioxide. For gas volumes further from the surface, the sensitivity to the reflective properties is much smaller (a few percent). The radiation budget of the black surface is nearly insensible to the opposite surface reflective properties for all the P_{CO_2} values considered (Table 3).

In the case of two highly reflective surfaces ($\epsilon_1 = \epsilon_2 = 0.1$), the diffuse / specular ratio for volumetric radiation budgets takes values close to those plotted in Fig. 9 and the surface radiation budgets are again not significantly modified. As already observed by Nelson (1979) for an isothermal gas volume, surface radiation budgets turn out to be independent of the reflective properties in the symmetric cases. However, gas radiation budgets appear significantly different in diffuse and specular cases, especially in the vicinity of high reflectivity surfaces.

Another important issue is the number of multiple reflections that need to be taken into account in order to attain a prescribed accuracy for systems with highly reflective surfaces. Again the illustration will make use of the 1m slab with two perfectly diffuse reflective surfaces ($\epsilon_1 = \epsilon_2 = 0$) and rather small absorber concentrations. Let $\zeta(i, j; r)$ be the ratio of the NER between the i^{th} and the j^{th} gas layers via r reflections over the full NER $\psi(i, j)$. Since (for such highly reflective configurations and low absorber concentrations) the ratio $\zeta(i, j; r)$ is approximately identical for all gas layer pairs, only its average value $\zeta(r)$ will be considered. Figure 10 gives the evolution of $\zeta(r)$ versus the number of reflections for three P_{CO_2} values. For $P_{CO_2} = 10^{-4} atm$, 50% of the exchanges are due to the first 10 reflections; however it is of interest to notice that 10% of the exchanges are occurring via more than 100 reflections and 1% via more than 800 reflections. Of course, the number of reflections decreases strongly as soon as the surface emissivities are not strictly zero : for 0.1 emissivities with $P_{CO_2} = 10^{-4} atm$, the first 25 reflections contribute to 99% of the average NER.

(d) Some validation tests. Three internal consistency tests were performed. The first one consists simply in the simultaneous development and intercomparison of two independent codes (Cherkaoui 93, Fournier 94).

The second set of tests relates to the way reflections are handled. A double simulation is performed : one with two black surfaces, the other with a black surface facing a specular reflective surface (reflectivity ρ). It can be shown that, if the temperature is continuous at the gas/surface interface, the limit value of the volumetric radiation budget at the reflective wall is $1+\rho$ times the radiation budget in the two black wall case. Especially, the multiplication factor is two in the $\rho = 1$ case, simply because the gas "sees" twice the system, directly and through a "mirror" reflection. We effectively controlled that our computations satisfied this property within the statistical errors ($< 1\%$).

The last test relates to the truncation error estimate in case of large numbers of multiple reflections. As shown in Sec. IV of (Cherkaoui et al., 1996), the truncated volumetric radiation budget is an under estimate of the solution; moreover adding to it the truncation error yields an overestimate (Eq.(32)). Both under and over estimates have to converge when the number of considered reflections increases to infinity. Test runs with two highly reflective surfaces did confirm the under and over estimation properties of these two quantities; convergence is achieved without any noticeable bias even for several hundred reflections (Fig. 11). This insures that the truncation error estimation remains valid when increasing the number of reflections. Also to be mentioned is the fact that the over estimate converges rapidly to the final solution. This property was observed for all optically thin cases : after a large enough number of reflections, the truncation estimation is nearly exact.

(e) Precision and computation times. The MCM allows an estimation of the confidence interval for each computed result. This estimation is based on the weighting factor variance as detailed in Sec. III. of (Cherkaoui et al., 1996) Checks were performed for bundle numbers ranging from a few ten to a few thousand per pair. The exact solution is "almost surely" within two standard deviations from the estimated integral, in coherence with the 95% confidence level expected for a normal distribution. It was also checked that the decreasing of the standard deviation with the number N of bundles followed the theoretical law in $\frac{1}{\sqrt{N}}$.

Table 4 contains the CPU times for nine typical configurations. In order to illustrate the increase in computation speed compared to AMCM requirements, we give in Fig. 12 the comparison of EMCM's computation times and those obtained with the AMCM code previously detailed by (Cherkaoui et al., 1992) with and without centering. In this centering technique, computed fluxes are offset by corresponding fluxes in the isothermal case. The numbers of bundles drawn are adjusted in order to obtain the required precision. As varied discretization cannot be addressed by the analogue code, the computations displayed in Fig. 12 are performed on a uniform discretization grid.

These results confirm those of Liu and Tiwari (1994) illustrating the fact that the MCM can be a computationally efficient tool for the simulation of gas radiative heat transfer. The EMCM allows us to go further in three different ways :

i) it allows much faster computations.

ii) the computation times are quasi identical for a regular or an extremely varied discretization grid.

iii) it is operational for both optically thin and optically thick systems.

It is worth reminding that the results of computations in Table 4 and Fig. 12 account for non-uniform temperature profiles within each gas layer. Displayed order of magnitude could be significantly lowered when taking the isothermal cell approximation.

(f) Conclusions. The Exchange Monte Carlo method (EMCM) is based on the notion of radiation net-exchange rate (NER), which insures an intrinsic fulfillment of the reciprocity principle. The resulting gain over Analogue Monte Carlo methods is very significant, particularly for nearly isothermal configurations : computations are a few orders of magnitude faster, strongly non-uniform discretizations introduce no specific convergence difficulties and numerical efficiency is little dependent on the system optical thickness. Another interesting feature is the possibility of easily partitioning the computations : the net-exchange rate between two cells can be computed without solving the whole radiative heat transfer problem. In addition to the intrinsic parallelization potential of Monte Carlo methods, this point should be an interesting property in term of massive parallel machine implementation.

The spectral aspects of gas radiation have been modeled with a narrow band statistical model. The Net-Exchange Formulation (NEF) being insensitive to spectral correlation effects, multiple reflections could be simulated without further approximations. Some results for high temperature configurations were compared to the solutions available in the literature. Configurations at ambient temperature were investigated in more details. The evolution of the volumetric radiation budgets as a function of surface emissivities and reflection properties was accurately determined for a wide range of absorbing species concentration. As far as our initial objectives are concerned, related to natural convection experiments in dwelling rooms, the simulation results showed that the volumetric radiation budgets were typically of the order of $1W.m^{-3}$. They are therefore not negligible compared to other heat transfer modes.

Finally, the same formal approach has been further used in other investigations. To be mentioned is the use of such an Exchange Monte Carlo method together with a k-distribution method. This proved to be especially efficient and allowed the simulation of two-dimensional configurations with acceptable computational costs (Fournier, 1994). Moreover, a linearized version of the Net-Exchange Formulation enables the coupling of the Monte Carlo code with finite volume techniques for simulations of coupled heat transfer processes (Cherkaoui (1993) and Fournier (1994)).

Additional References

Cherkaoui, M., Dufresne, J. L., Fournier, R., Grandpeix, J. Y., Lahellec, A, 1996, "Monte Carlo Simulation of Radiation in Gases with a Narrow-Band Model and a Net-Exchange Formulation", ASME Journal of Heat Transfer, May 1996, Vol.118, pp.401-407

Nelson, D. A., 1979, "Band Radiation within Diffuse-Walled Enclosures, Part 1 : Exact Solutions for Simple Enclosures," ASME Journal of Heat Transfer, Vol. 101, pp. 81-84.

Soufiani, A.,1994, Private Communication, EM2C Laboratory (ECP-CNRS); Chatenay-Malabry; France.

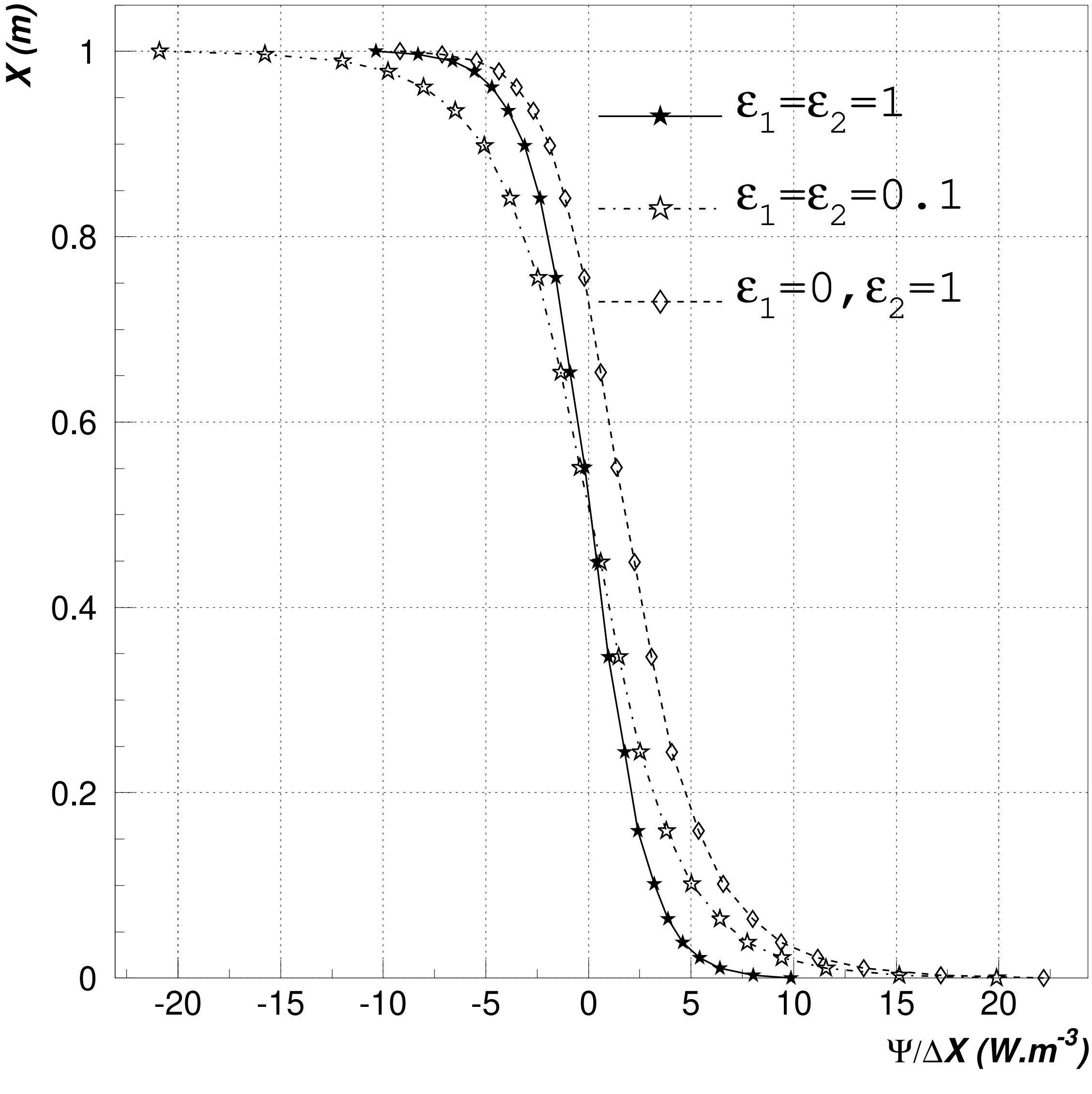

Figure 1: Volumetric radiation budget for pure CO_2 ($P_{CO_2} = 1atm$) with a linear temperature profile varying from $295K$ at $S(1) = 0$ to $305K$ at $S(2) = 1m$. The various diffuse surface emissivities are : $\epsilon_1 = \epsilon_2 = 1$; $\epsilon_1 = \epsilon_2 = 0.1$; $\epsilon_1 = 0, \epsilon_2 = 1$.

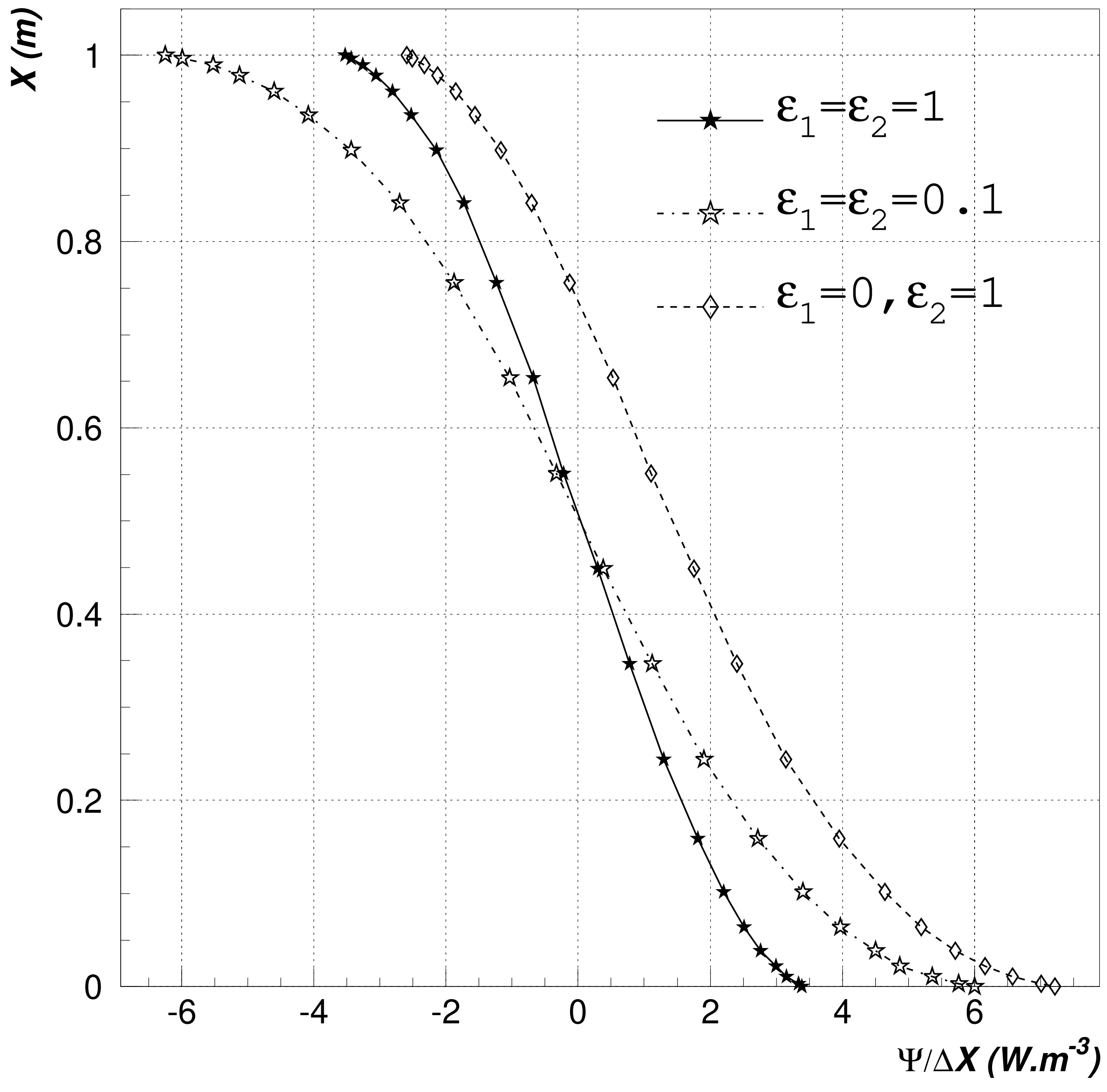

Figure 2: Same radiation budget as Fig. 1 for $P_{CO_2} = 10^{-2} atm$

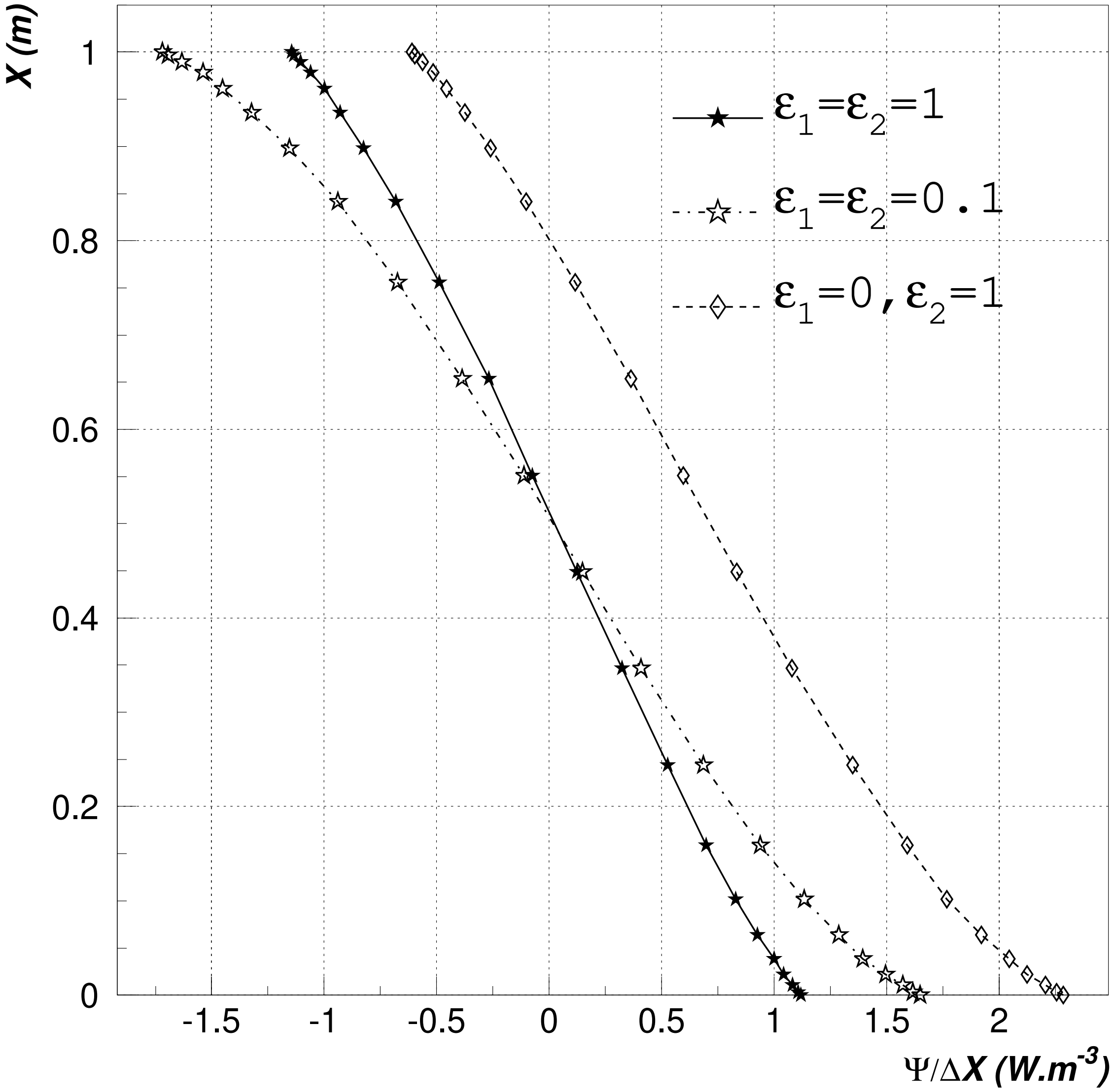

Figure 3: Same radiation budget as Fig. 1 for $P_{CO_2} = 10^{-3} atm$

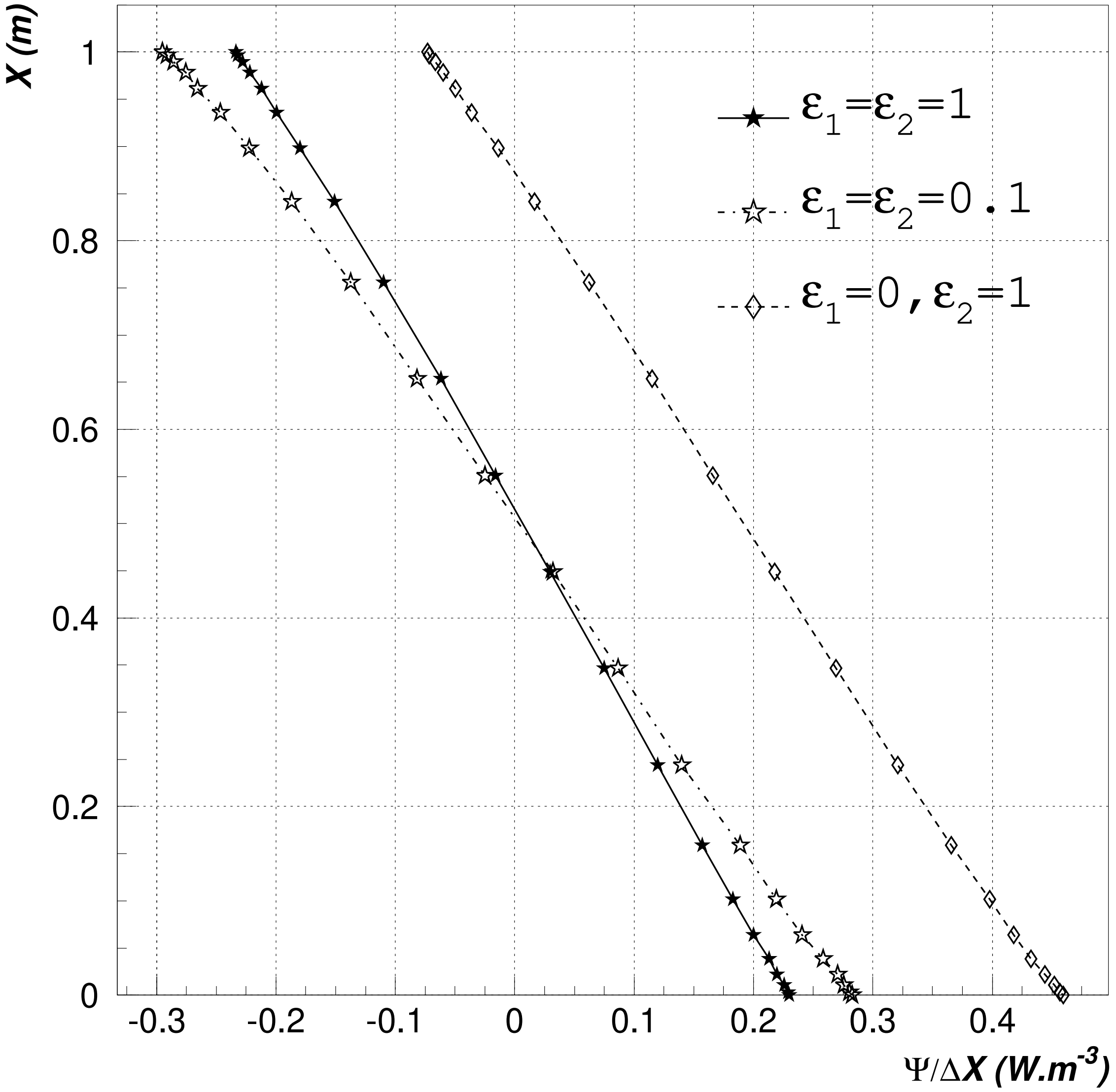

Figure 4: Same radiation budget as Fig. 1 for $P_{CO_2} = 10^{-4} atm$

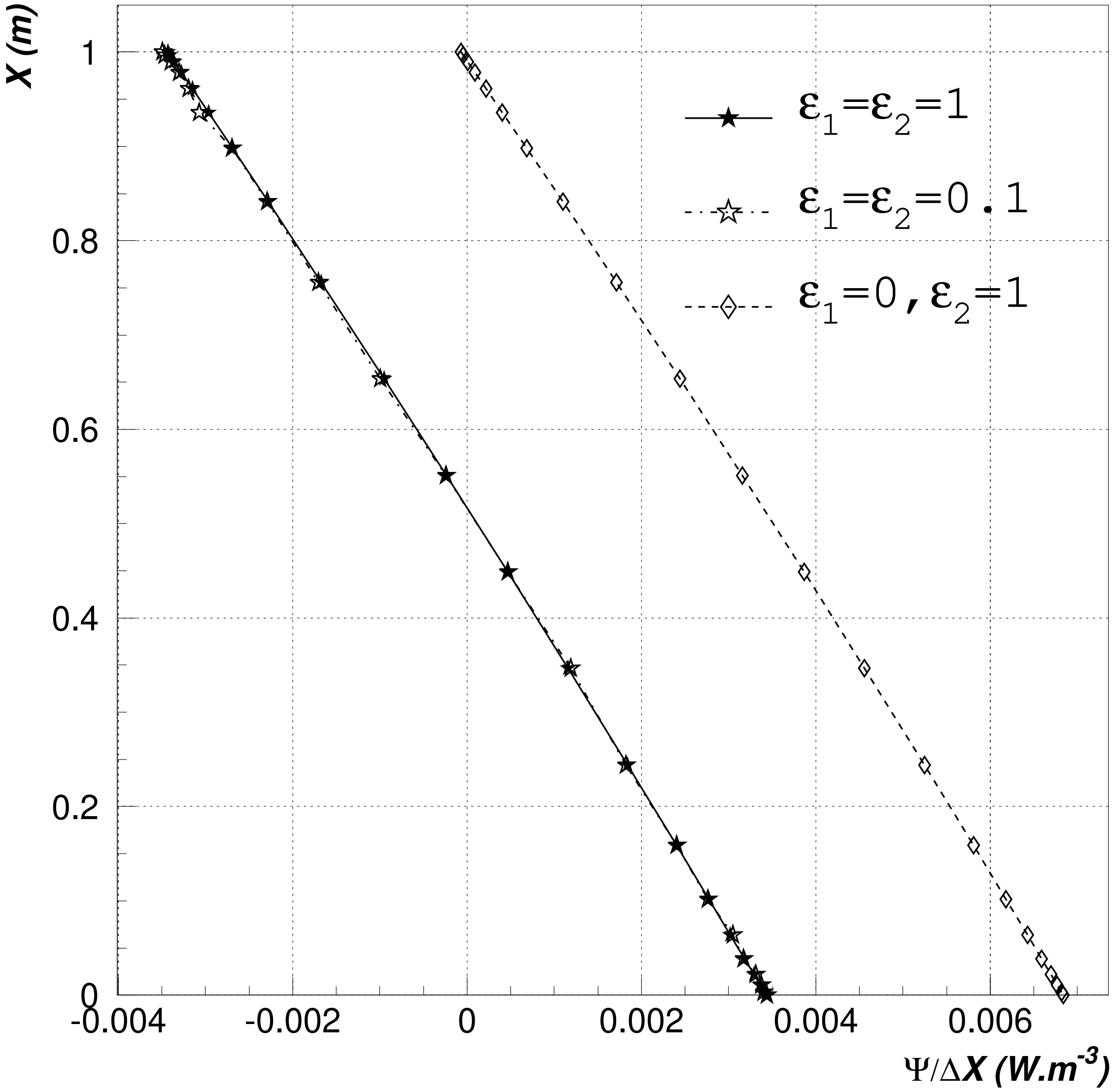

Figure 5: Same radiation budget as Fig. 1 for $P_{CO_2} = 10^{-6} atm$

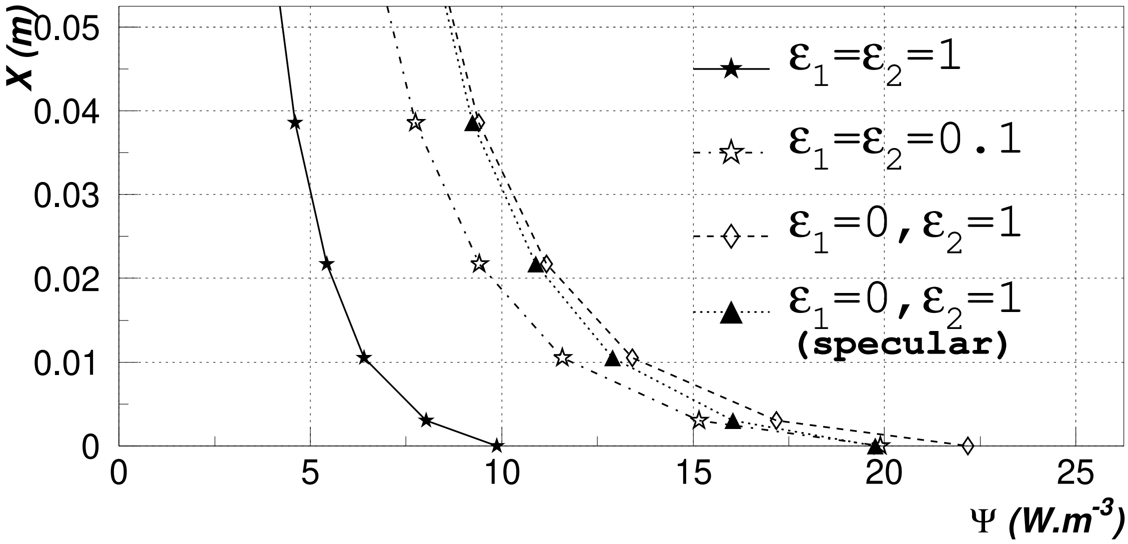

Figure 6: Radiation budget for the same configuration as Fig. 1 : detail close to the cold surface 1. When $\epsilon_1 = 0$ and $\epsilon_2 = 1$ the reflection is either diffuse or specular.

$Gas Layer$ Nb	$Gas Layer$ $thickness \Delta X/D$
1	0.000000
2	$0.599\ 10^{-2}$
3	$0.899\ 10^{-2}$
4	$1.348\ 10^{-2}$
5	$2.023\ 10^{-2}$
6	$3.034\ 10^{-2}$
7	$4.551\ 10^{-2}$
8	$6.826\ 10^{-2}$
9	$1.024\ 10^{-1}$
10	$1.024\ 10^{-1}$
11	$1.024\ 10^{-1}$

Table 1: Discretization ; gas layer thicknesses for half of the slab (symmetric grid).

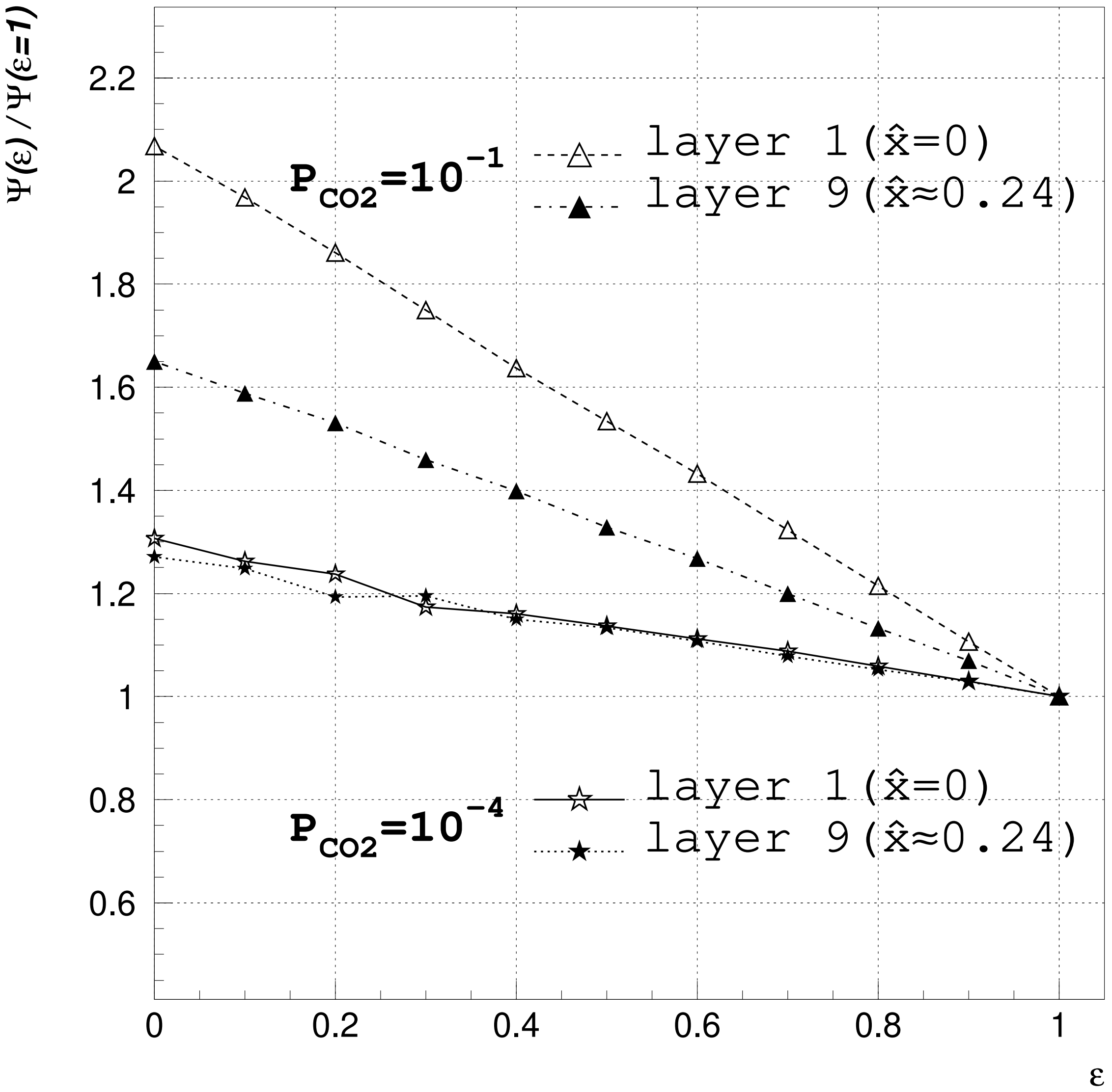

Figure 7: Ratio between the radiation budgets for diffuse reflecting surfaces of same emissivities ($\epsilon_1 = \epsilon_2 = \epsilon$) and those for black surfaces versus the surface emissivities (ϵ) for two specific layers and for two partial pressures of carbon dioxide ($P_{CO_2} = 10^{-4}atm$ and $P_{CO_2} = 10^{-1}atm$). The temperature profile is linear ($295K$ at $S(1) = 0$ to $305K$ at $S(2) = 1m$).

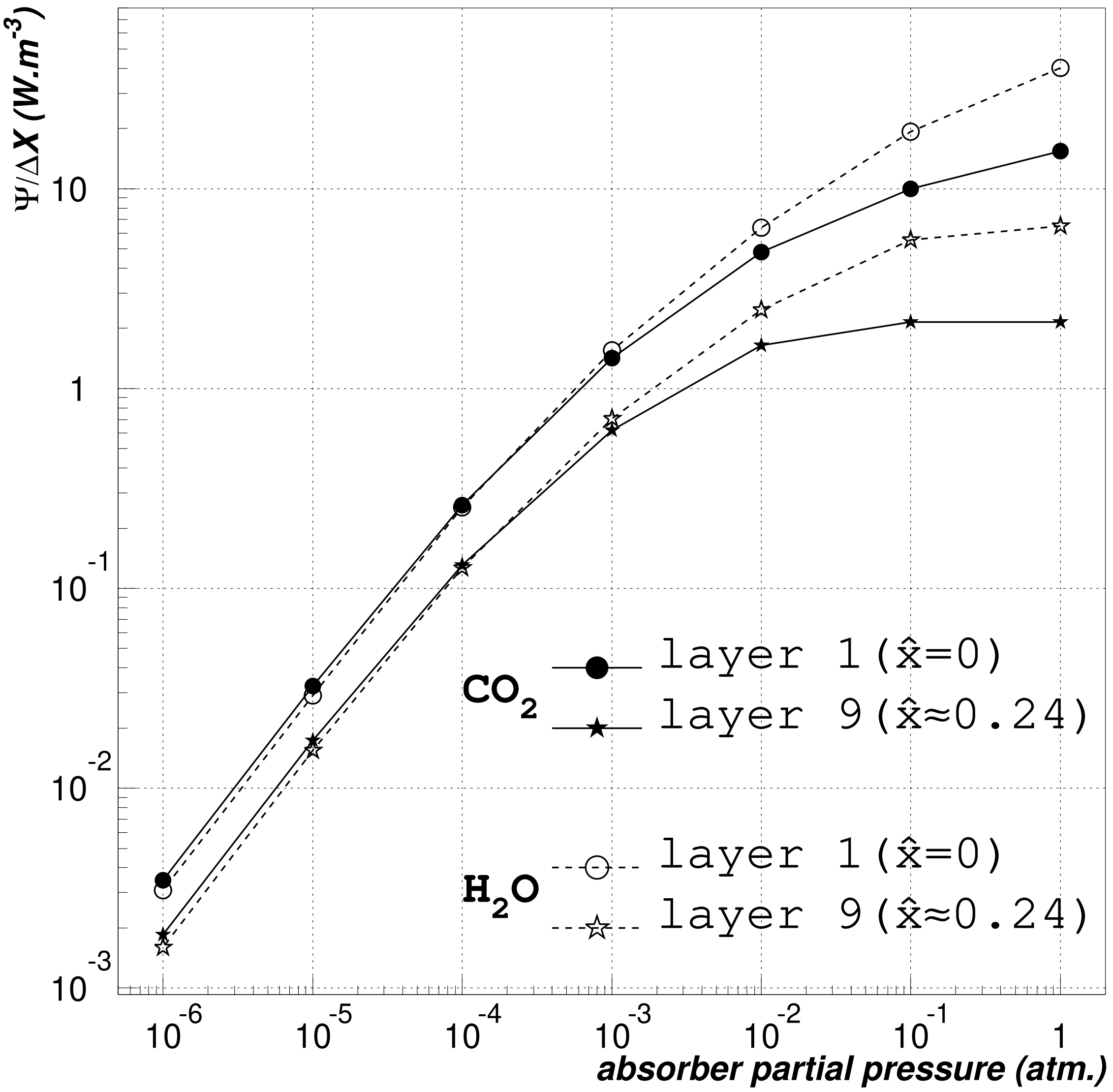

Figure 8: Radiation budget for two specific layers versus partial pressures of absorbing gas (CO_2 and H_2O) with a linear temperature profile ($295K$ at $S(1) = 0$ to $305K$ at $S(2) = 1m$) and diffuse reflecting surfaces ($\epsilon_1 = \epsilon_2 = 0.5$).

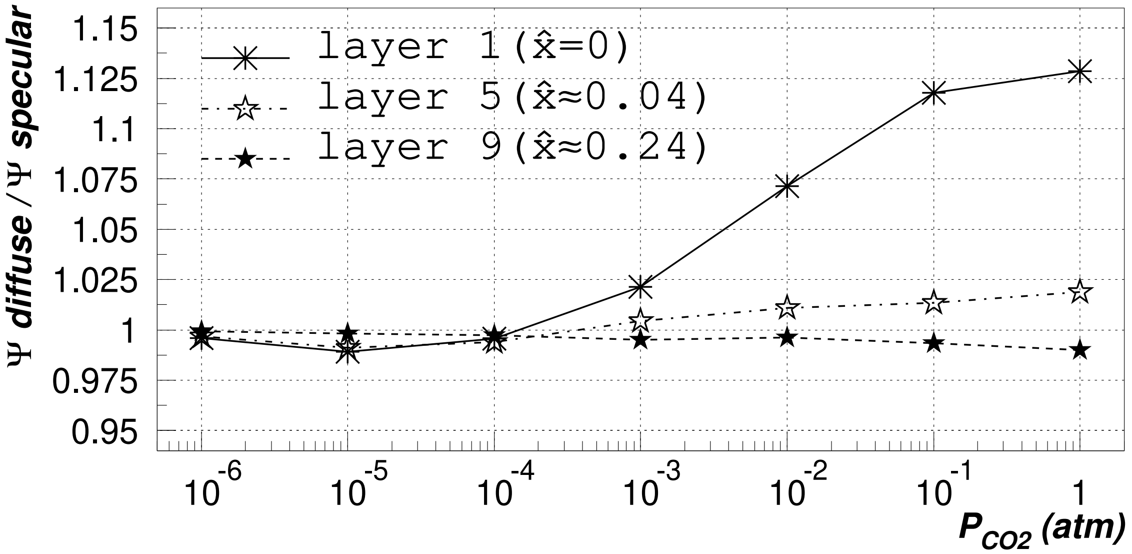

Figure 9: Ratio between the radiation budgets for diffuse reflections and those for specular reflections versus partial pressures of absorbing gas (CO_2), in the case of one perfectly reflective and one black surface ($\epsilon_1 = 0$, $\epsilon_2 = 1$). The temperature profile is linear ($295K$ at $S(1) = 0$ to $305K$ at $S(2) = 1m$).

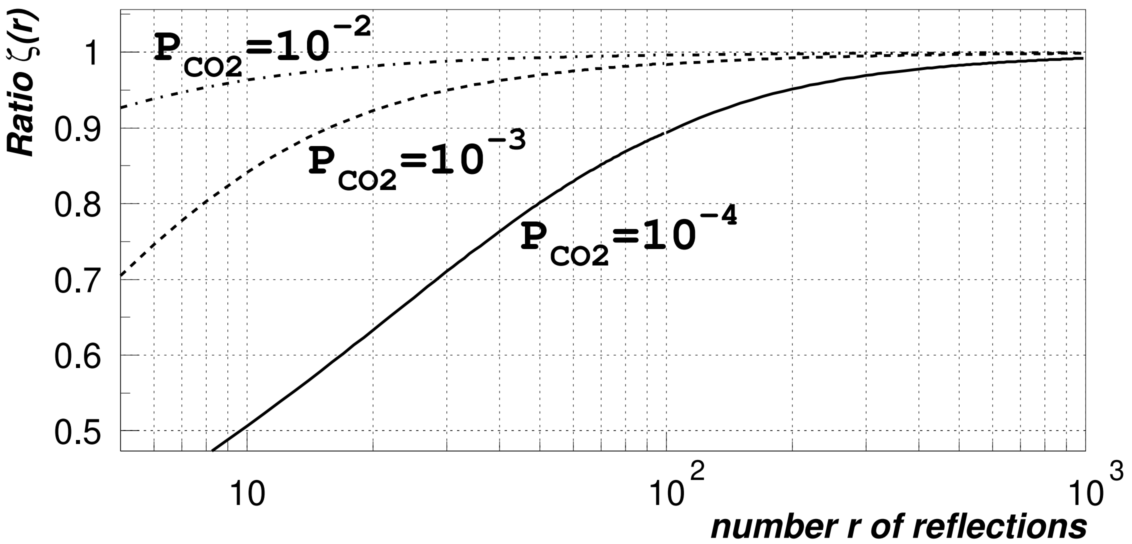

Figure 10: Ratio $\zeta(r)$ between the net-exchange rate through the r first reflections and the net-exchange rate through an infinite number of reflections as a function of r. The two surfaces are perfectly diffuse reflective ($\epsilon_1 = \epsilon_2 = 0$). The temperature profile is linear ($295K$ at $S(1) = 0$ to $305K$ at $S(2) = 1m$).

Figure 11: Under and over estimate of the radiation budget for a particular mesh (locat at $\approx 0.04m$ from $S(1)$) as a function of the number of reflection. $P_{CO_2} = 10^{-3}$, the two surfaces are perfectly specular reflective ($\epsilon_1 = \epsilon_2 = 0$), the temperature profile is linear ($295K$ at $S(1) = 0$ to $305K$ at $S(2) = 1m$).

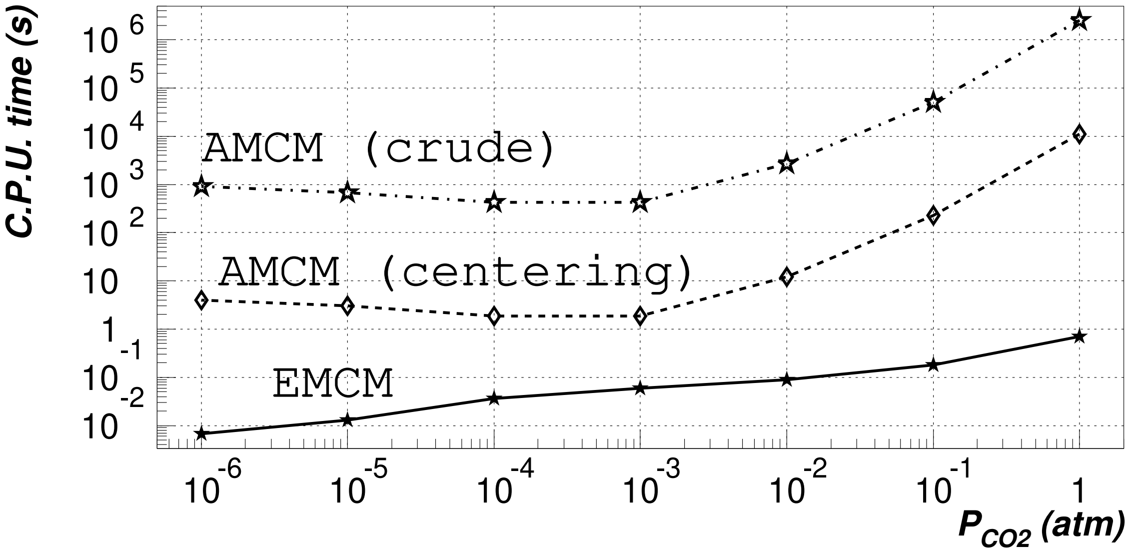

Figure 12: CPU time (with RNDM as random generator, on a 40 MFlops workstation HP-735) versus Carbon dioxide partial pressure for AMCM and EMCM. Bundles drawing are adjusted to get a statistical error lower than 5% on radiation budgets 15cm off the surfaces. Both surfaces are black ($\epsilon_1 = \epsilon_2 = 1$); temperature profile is linear from $295K$ at $S(1) = 0$ to $305K$ at $S(2) = 1m$; the gas medium is regularly discretized into 10 layers.

Gaz	θ^s (K)	ϵ_1	ϵ_2	D (m)	$\psi^s(1)$ $(kW.m^{-2})$	$\psi^s(2)$ $(kW.m^{-2})$	volumetric radiation budget at center $(kW.m^{-3})$
pure H_2O	0.	1.	1.	1.	28.094 ± 0.015	$-$	-23.17 ± 0.04
				0.5	24.26 ± 0.01	$-$	-50.07 ± 0.07
				0.1	14.417 ± 0.005	$-$	-219.6 ± 0.4
		0.1	1.	0.5	2.425 ± 0.004	28.00 ± 0.01	-34.40 ± 0.06
pure H_2O	500.	0.5	0.5	1.	4.700 ± 0.004	$-$	-4.917 ± 0.012
				10^{-1}	2.473 ± 0.002	$-$	-43.08 ± 0.08
($3755cm^{-1}$				10^{-2}	0.6594 ± 0.0004	$-$	-130.0 ± 0.2
bande		0.1	0.1	1.	1.160 ± 0.002	$-$	-1.410 ± 0.005
only)				10^{-1}	0.7755 ± 0.0007	$-$	-14.08 ± 0.04
				10^{-2}	0.3448 ± 0.0003	$-$	-68.17 ± 0.15
pure CO_2	500.	0.5	0.5	1.	1.709 ± 0.002	$-$	-1.278 ± 0.004
				10^{-1}	1.094 ± 0.001	$-$	-18.05 ± 0.04
($3715cm^{-1}$				10^{-2}	0.3379 ± 0.0002	$-$	-66.09 ± 0.11
bande		0.1	0.1	1.	1.278 ± 0.004	$-$	-0.3395 ± 0.0018
only)				10^{-1}	18.05 ± 0.04	$-$	-5.175 ± 0.017
				10^{-2}	66.09 ± 0.11	$-$	-31.48 ± 0.08

Table 2: Surface radiation budget at the walls and volumetric radiation budget at center for high temperature configurations ($\theta^g = 1000K$, $\theta^s_1 = \theta^s_2 = \theta^s$)

emissivities Surface	Hot Wall Radiation Budget $\psi^s(2)$ $(W.m^{-2})$			
	Carbone dioxyde			
	$P_{CO_2} = 1$	$P_{CO_2} = 10^{-2}$	$P_{CO_2} = 10^{-3}$	$P_{CO_2} = 10^{-6}$
$\epsilon_1 = \epsilon_2 = 1$	-52.60	-58.82	-60.56	-61.24
$\epsilon_1 = \epsilon_2 = 0.5$	-17.82	-19.81	-20.28	-20.415
$\epsilon_1 = \epsilon_2 = 0.1$	-2.835	-3.143	-3.203	-3.223
$\epsilon_1 = \epsilon_2 = 0.1, specular$	-2.851	-3.161	-3.211	-3.223
$\epsilon_1 = 0,\ \epsilon_2 = 1$	-2.145	-1.590	-0.7401	$-3.469\ 10^{-3}$
$\epsilon_1 = 0,\ \epsilon_2 = 1, specular$	-2.153	-1.597	-0.7404	$-3.463\ 10^{-3}$
	Water vapor			
	$P_{H_2O} = 1$	$P_{H_2O} = 10^{-2}$	$P_{H_2O} = 10^{-3}$	$P_{H_2O} = 10^{-6}$
$\epsilon_1 = \epsilon_2 = 1$	-38.83	-58.09	-60.49	-61.24
$\epsilon_1 = \epsilon_2 = 0.5$	-13.78	-19.70	-20.27	-20.42

Table 3: Hot plate radiation budget for various surface emissivities and various partial pressures of absorbing gases (CO_2 and H_2O) with a linear temperature profile ($295K$ at $S(1) = 0$ to $305K$ at $S(2) = 1m$).

P_{CO_2}	1			10^{-3}			10^{-5}		
ϵ	1.	0.5	0.1	1.	0.5	0.1	1.	0.5	0.1
CPU time (s)	1.9	4.0	7.4	0.13	0.8	1.4	1.4	8.	65.
N^{ss}	510	290	290	10	10	10	170	150	125
N^{sg}	510	290	290	200	200	100	1700	1500	2500
N^{gg}	510	290	290	10	10	10	170	150	125

Table 4: Number of realizations for each pair of cells (N^{ss} for surface-surface exchanges, N^{gs} for gas-surface exchanges and N^{gg} for gas-gas exchanges) and total CPU times (with RNDM as random generator, on a 40 MFlops workstation HP-735) for a 5% statistical error ; linear temperature profile from $295K$ at $S(1) = 0$ to $305K$ at $S(2) = 1m$; $\epsilon_1 = \epsilon_2 = \epsilon$; discretization of Table 1; truncation error lower than 3% in case of reflective surfaces.